

Research Article

Evaluation of Poly(2-Ethyl-2-Oxazoline) Containing Copolymer Networks of Varied Composition as Sustained Metoprolol Tartrate Delivery Systems

Bistra Kostova,^{1,4} Sijka Ivanova,² Konstantin Balashev,³ Dimitar Rachev,¹ and Darinka Christova^{2,4}

Received 17 January 2014; accepted 31 March 2014; published online 3 May 2014

Abstract. Segmented copolymer networks (SCN) based on poly(2-ethyl-2-oxazoline) and containing 2-hydroxyethyl methacrylate, 2-hydroxypropyl acrylate, and/or methyl methacrylate segments have been evaluated as potential sustained release systems of the water soluble cardioselective β -blocker metoprolol tartrate. The structure and properties of the drug carriers were investigated by differential scanning calorimetry, attenuated total reflectance Fourier transform infrared spectroscopy, scanning electron microscopy, and atomic force microscopy. Swelling kinetics of SCNs in various media was followed, and the conditions for effective MT loading were specified. MT-loaded SCNs with drug content up to 80 wt. % were produced. The release kinetics of metoprolol tartrate from the systems was studied and it was shown that the conetworks of different structure and composition are able to sustain the metoprolol tartrate release without additional excipients.

KEY WORDS: drug delivery; metoprolol tartrate; polyoxazolines; segmented copolymer networks.

INTRODUCTION

A main priority of the contemporary polymer science and pharmaceutical technology is to improve the targeting properties and the efficiency of controlled release systems. Hence, the research has focused on the synthesis of new polymer carriers and optimization of the properties of present drugs with improved functionality, bioavailability, and safety delivery. In clinical and pharmaceutical practices, the water soluble polymers cover vast areas of applications (1, 2). Along with the widely used polymers in the development of drug formulations such as poly(ethylene glycol) (PEG) (3–5), poly(vinyl pyrrolidone) (6, 7), poly(vinyl alcohol) (8, 9), poly(acrylic acid) (10, 11), and polyphosphoesters (12, 13), poly(2-oxazoline)s are currently considered as versatile materials for polymer therapeutics (14–16). This class of polymers meets all specific requirements needed for the development of drug carriers such as biocompatibility, solubility, wide range of chemical functionality, and chain architectures. Poly(2-oxazoline)s are synthesized by living cationic ring-opening polymerization of 2-substituted-2-oxazolines and physicochemical properties depend on the substituent in the oxazoline ring, as well as the macromolecular structure and

composition (17–19). In order to modify the properties and further enlarge the area of potential applications of poly(2-oxazolines), the efforts are directed towards the synthesis of various block and star copolymers, segmented copolymer networks (also known as conetworks), and so on (20–23). However, the use of poly(2-alkyl-2-oxazolines) in drug delivery so far is not well covered, and the research is focused mainly on the systems which increase the solubility of hydrophobic drugs. Luxenhofer *et al.* reported for the synthesis of di- and tri-block copolymers based on poly(2-oxazolines) for the solubilization of water-insoluble drugs (24). Han Y. *et al.* used amphiphilic poly(2-oxazoline)s micelles as a promising high-capacity delivery platform carrying synergistic combinations of multiple chemotherapeutic agents for multidrug cancer chemotherapy. Multidrug (paclitaxel, docetaxel, 17-allylamino-17-demethoxygeldanamycin, etoposide, and bortezomib) loaded poly(2-oxazoline)s micelles showed enhanced stability and improved drug delivery characteristics (25). Guillerme *et al.* applied a copper-catalyzed azide-alkyne Huisgen's cycloaddition click reaction to obtain graft copolymers from poly(ϵ -caprolactone) and poly(2-methyl-2-oxazoline) homopolymers that could be used as potential drug carriers (26). El-Hag Ali and AlArifi utilized γ -rays induced polymerization and cross-linking to obtain a series of pH-sensitive hydrogels on the basis of poly(2-ethyl-2-oxazoline) (PEtOx) and acrylic acid (27). In a previous paper, we have reported on the synthesis and properties of amphiphilic conetworks comprising of PEtOx, 2-hydroxyethyl methacrylate, and hydroxypropyl acrylate segments as new platforms for drug delivery. These networks loaded with the hydrophobic drug ibuprofen showed high drug loading efficiency and ability to sustain the ibuprofen release more than 8 h (28).

¹Department of Pharmaceutical Technology and Biopharmaceutics, Faculty of Pharmacy, Medical University - Sofia, 2 Dunav Str., Sofia, 1000, Bulgaria.

²Institute of Polymers, Bulgarian Academy of Sciences, Akad. G. Bonchev Str. Bl. 103A, Sofia, 1113, Bulgaria.

³Faculty of Chemistry and Pharmacy, Sofia University, 1 James Bourchier Ave., Sofia, 1164, Bulgaria.

⁴To whom correspondence should be addressed. (e-mail: bistrakostova@abv.bg; dchristo@polymer.bas.bg)

The aim of this work is to study the potential of the segmented copolymer networks (SCNs) based on PEtOX as drug delivery carriers for hydrophilic, well water soluble drug molecules. When aiming a prolonged and controlled release, the extremely high solubility of the therapeutic substance in aqueous media represents considerable technological challenge. The ability to implement effective control over the release of kinetics in such case can be achieved only through precise selection of the polymeric carrier, e.g., by using amphiphilic polymers, copolymers, or networks with proper combination of hydrophilic and hydrophobic segments. SCNs are appropriate for the purpose as they possess porous morphology and chemical structure that could be varied in a wide range of properties. It is expected that by varying the copolymer composition and hydrogel morphology, it will be possible to influence the drug loading capacity of SCNs and subsequently to control the drug release kinetics. For this purpose, a series of PEtOX-based copolymer networks of varied hydrophilic/hydrophobic balance and cross-linked density were loaded with metoprolol tartrate (MT) as a model drug. MT represents extremely well soluble and highly permeable cardioselective β -blocker from class I of Biopharmaceutics Classification System (BCS) (29).

The characteristics of MT-loaded systems were studied by swelling at different conditions, differential scanning calorimetry (DSC), Fourier transform infrared spectroscopy (FTIR), scanning electron microscopy (SEM), and atomic force microscopy (AFM). *In vitro* drug dissolution studies were carried out in order to estimate the potential of the developed systems for sustained MT delivery.

EXPERIMENTAL SECTION

Materials

2-Ethyl-2-oxazoline, acrylic acid, 2-hydroxyethyl methacrylate, hydroxypropyl acrylate, and methyl methacrylate (all purchased from Sigma-Aldrich) were purified according to the known procedures. Metoprolol tartrate EP was supplied by Indukern Chemie (Schlieren, Switzerland). PBS tablets (phosphate buffered saline, pH 6.8) were purchased from Sigma-Aldrich. All other reagents and solvents were used as received, unless otherwise specified.

SCNs were prepared by UV-induced radical copolymerization of poly(2-ethyl-2-oxazoline)- α,ω -diacrylate with corresponding comonomers (2-hydroxyethyl methacrylate, hydroxypropyl acrylate, and methyl methacrylate) as described previously (23, 30). The PEtOX- α,ω -diacrylate was synthesized according to the earlier reported procedure (31). The main characteristics of the macromer used in this work are as follows (values obtained by ^1H NMR in CDCl_3): number average molar mass of 10,200 g/mol and end-group functionality (i.e., average number of acrylate end groups per macromolecule) of 1.98.

The synthesized SCNs were purified by extraction with ethanol and deionized water, and dried in vacuum until constant weight. The calculated soluble fractions were lower than 4% which proved copolymer compositions close to the theoretical ones.

Drug Loading

Test samples for drug loading experiments were prepared by cutting uniform disks (diameter 6 ± 0.01 mm; thickness 1 ± 0.05 mm) from the dry SCN films. The disks were immersed for 24 h in water solution of MT of concentration 240 mg/mL. Then, the SCN platforms swollen to equilibrium were carefully taken out, the excess of the solution on the surface was removed by blotting with filter paper, and the disks were dried under vacuum to a constant weight.

The amount of loaded drug for each sample was calculated from the weight of the dry sample before and after loading.

SCN Swelling Kinetics

Swelling kinetics of the SCN films was followed by: (i) deionized water at 20°C and (ii) buffer solution with pH 6.8 at 37°C. Typical procedure was as follows: Disk cut from the SCN films was dried under vacuum until constant weight was attained. The disk was transferred to the test tube containing corresponding swelling media. At regular intervals, the disk was taken out, the excess solvent was removed from the surface with tissue paper, the disc's weights were registered, and the disc then returned to the medium. The swelling was continued until a constant weight was attained. The equilibrium swelling degree, Q , was calculated from the equation below, where W_d is the initial weight of the dry sample and W_s is the weight of the sample swollen to equilibrium.

$$Q(\%) = \frac{W_s - W_d}{W_d} \times 100$$

Fourier Transform Infrared Spectroscopy

Attenuated Total Reflectance Fourier Transform Infrared (ATR-FTIR) spectra were recorded using an IRAffinity-1 spectrophotometer (Shimadzu Co., Kyoto, Japan) equipped with a MIRacle™ ATR accessory (diamond crystal; PIKE Technologies, USA) providing depth of penetration of the IR beam into the sample of about 2 μm . SCN samples were scanned over wavenumber range of 4,000–500 cm^{-1} before and after MT loading. Fifty scans were performed at a resolution of 4 cm^{-1} .

Differential Scanning Calorimetry

Differential scanning calorimetry (DSC) analysis was carried out on Perkin-Elmer DSC 8500 equipment. The samples were analyzed in the temperature range from -20 to 160°C at scanning rate of $10^\circ\text{C}/\text{min}$ in nitrogen atmosphere.

Scanning Electron Microscopy (SEM)

The scanning electron micrographs were taken on a JEOL JSM-5510 (Japan). Prior to analysis, the samples were frozen in liquid nitrogen, fractured, and then freeze-dried. All SEM images were obtained from the gold-coated cross-section surfaces (Sputter Coater Jeol Fine Coater 1200, Japan) using 6 to 10 kV electron energy beams.

Atomic Force Microscopy (AFM)

AFM imaging was performed on NanoScope MultiMode V system (Bruker Inc., Germany), operating in tapping mode in air at room temperature. The setup uses a fixed probe which in tapping mode is piezoelectrically driven to oscillate. The sample is glued by double-side tape on a round metal disk (“puck”), which is magnetically attached to the top of the scanner tube. The latter translates the sample back and forth horizontally, while the probe extracts information from the deflection of the cantilever as the tip encounters the surface. The return signal reveals information about the vertical height of the sample surface and some other features of the deposited on mica material. The silicon cantilevers (Tap 300 Al-G, Budget Sensors, Innovative solutions Ltd, Bulgaria) were used with 30-nm-thick aluminum reflex coating. The cantilever spring constant was in the range of 1.5–15 N/m and the resonance frequency was 150 ± 75 kHz. The tip radius was less than 10 nm. Before imaging, the samples were thoroughly blown with N_2 gas to remove any contaminants and moisture. The scan rate was set at 1 Hz, and the images were captured in the height and phase modes with 512×512 pixels in a JPEG format. Subsequently, all images were flattened by means of the Nanoscope’s software (v.7.30). The samples were scanned in several different locations along the surface.

In Vitro Drug Dissolution Studies

Drug release kinetics were evaluated using a dissolution test apparatus (Erweka DT 600, Hensenstmm, Germany). The USP basket method was selected. The test was carried out at basket rotation speed of 100 rpm, maintained at $37 \pm 0.5^\circ\text{C}$, in 500-mL dissolution medium at pH value of 6.8. The dissolution progress was monitored by withdrawing 5-ml filtered samples ($0.45 \mu\text{m}$ filter) at preselected intervals (up to 8 h). The content of MT in the sample solutions was determined by measuring the UV absorbance of the samples at 278 ± 2 nm using a Hewlett-Packard 8452 A Diode Array spectrophotometer (New Jersey, USA). The cumulative percentage of drug release was calculated, and the average of six determinations was used in the data analysis. The standard deviations did not exceed to 2%.

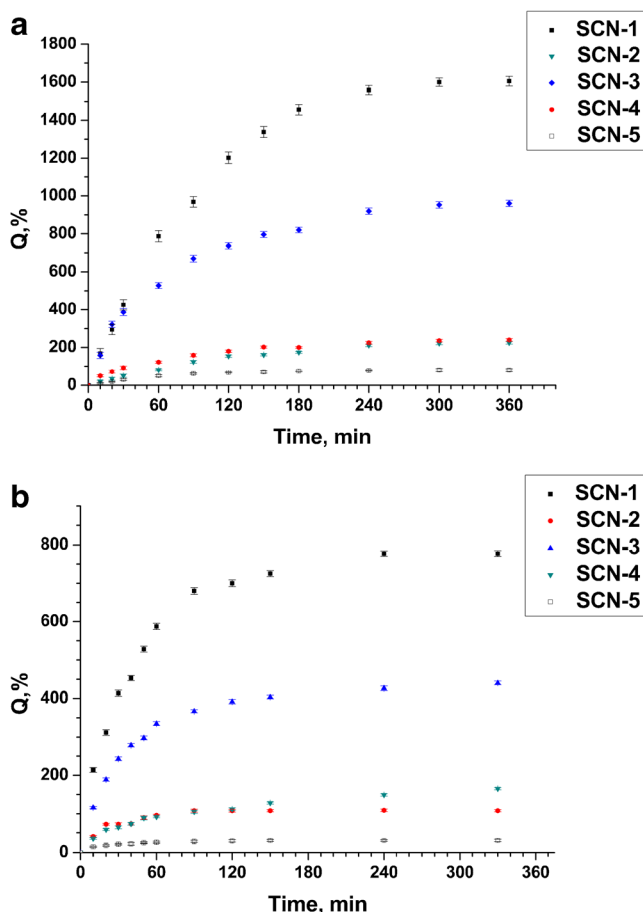


Fig. 1. Swelling kinetics of the conetworks in: (a) deionized water at 20°C ; (b) buffer solution (pH 6.8) at 37°C

RESULTS AND DISCUSSION

Synthesis and Characterization of the SCN Drug Carriers

SCNs were synthesized in a form of 1-mm-thick films according to the previously reported procedure (28), by using UV-induced radical copolymerization of poly(2-ethyl-2-oxazoline)- α,ω -diacrylate with (meth)acrylate comonomers such as 2-hydroxyethyl methacrylate (HEMA), hydroxypropyl acrylate

Table I. SCN Swelling Characteristics and Drug Loading

Code	Composition	Swelling, %			MT loading, %		Average MT content, mg
		Equilibrium swelling in water	Equilibrium swelling in BS pH 6.8	Swelling in aqueous MT	*Based on weight	** Based on swelling	
SCN-1	PHEMA ₃₀ -l-PEtOx ₇₀	1,605	780	1,930	84.19	82.27	135.8 \pm 3.4
SCN-2	PHEMA ₇₀ -l-PEtOx ₃₀	225	110	740	64.95	64.09	83.0 \pm 1.8
SCN-3	PHPA ₃₀ -l-PEtOx ₇₀	960	440	1,350	77.26	76.42	131.5 \pm 3.0
SCN-4	PHPA ₇₀ -l-PEtOx ₃₀	240	165	760	64.57	64.51	91.7 \pm 2.2
SCN-5	P(HEMA ₃₀ -co-MMA ₅₀)-l-PEtOx ₂₀	80	30	320	46.58	43.43	69.6 \pm 1.9

MT metoprolol tartrate; PEtOx poly(2-ethyl-2-oxazoline)

*Calculations based on weight

**Calculations based on swelling of SCN in MT aqueous solution of concentration 240 g/L for 24 h

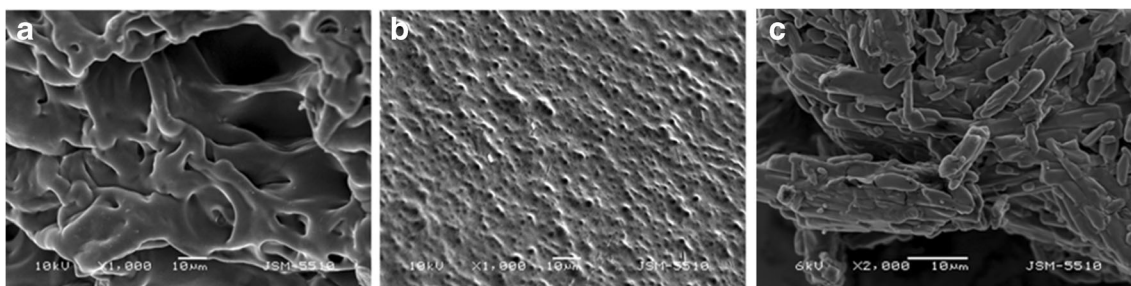


Fig. 2. SEM images of: (a) fracture of pure SCN-3 swollen in water to the equilibrium and freeze-dried; (b) fracture of SCN-3 swollen to the equilibrium in aqueous solution of MT and freeze-dried; (c) pure MT substance

(HPA), and methyl methacrylate (MMA). Discs with the diameter of 0.6 cm were cut and used as test samples for characterization, drug loading, and dissolution experiments. The swelling characteristics of the developed drug carriers are summarized in Table I and in Fig. 1.

The swelling experiments held in different media revealed the decisive influence of the copolymer composition on the SCN properties. It is clear that samples with high PEtOx content (SCN-1 and SCN-3) show impressive swelling kinetics in both water and PBS, and reach much higher equilibrium swelling degrees compared to the SCNs of the same constituents but with lower PEtOx content (SCN-2 and SCN-4). SCN-1 reached 1,600% equilibrium swelling for a period of 5 h; while for the same time, SCN-2 absorbed only 200%. Similarly, SCN-3 reached 980% swelling in water for 5 h, while SCN-4 only absorbed 220%. Therefore, one may conclude that swelling of these materials in aqueous media strongly depends not only on the PEtOx content, but also on the comonomer type and content. As expected, the ternary SCN-5 which contains hydrophobic PMMA segments showed the lowest swelling degree in water. The swelling behavior of the studied conetworks in water is very important in view of the subsequent drug loading process.

The high swelling capacity is expected to contribute to a high MT loading as well.

On the other hand, swelling of the studied SCNs in buffer solution (pH 6.8) at physiological temperature could elucidate the potential of these networks to control the release of hydrophilic drugs. The swelling kinetics of the SCNs in PBS at 37°C is presented in Fig. 1b. It is clear that swelling behavior in buffer solution is similar to that in water as all SCNs swelling kinetics follow the same course. However, equilibrium swelling degrees of the networks at pH 6.8 are about 50% lower compared to the corresponding swelling in deionized water. This indicates that the buffer solution causes significant collapse of the SCN structure. This is a very important result which implies that the investigated PEtOx copolymers can be assigned to the smart polymeric carriers suitable for prolonged and controlled drug release systems. High swelling in water at 20°C allows SCNs to be loaded with water soluble drug, whereas the partial collapse at pH 6.8 and 37°C enables the controlled drug release over a period of time. Although all SCNs follow the same swelling course, they show significant differences in the equilibrium swelling degrees depending on

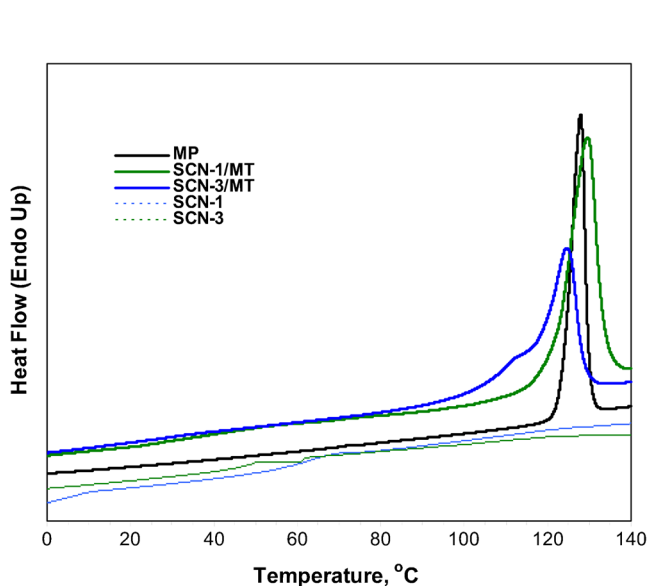


Fig. 3. DSC thermograms (first heating) of systems SCN-1 and SCN-3 loaded with MT compared to the thermogram of pure MT

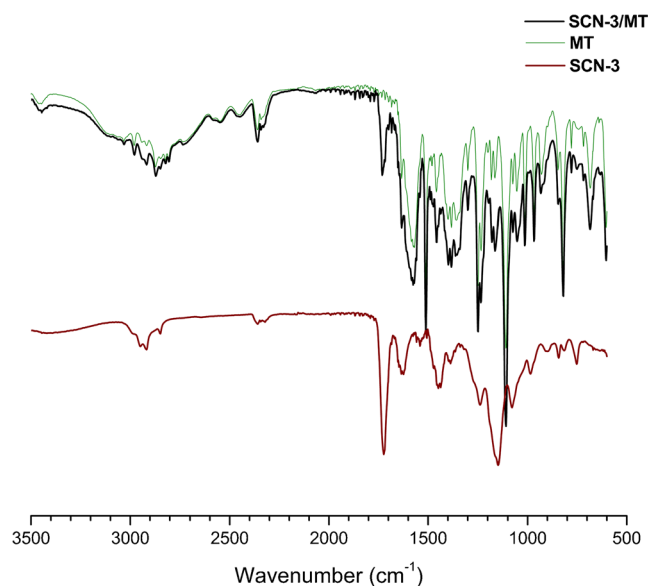


Fig. 4. FTIR spectra of SCN-3 and SCN-3/MT compared to the spectrum of pure MT

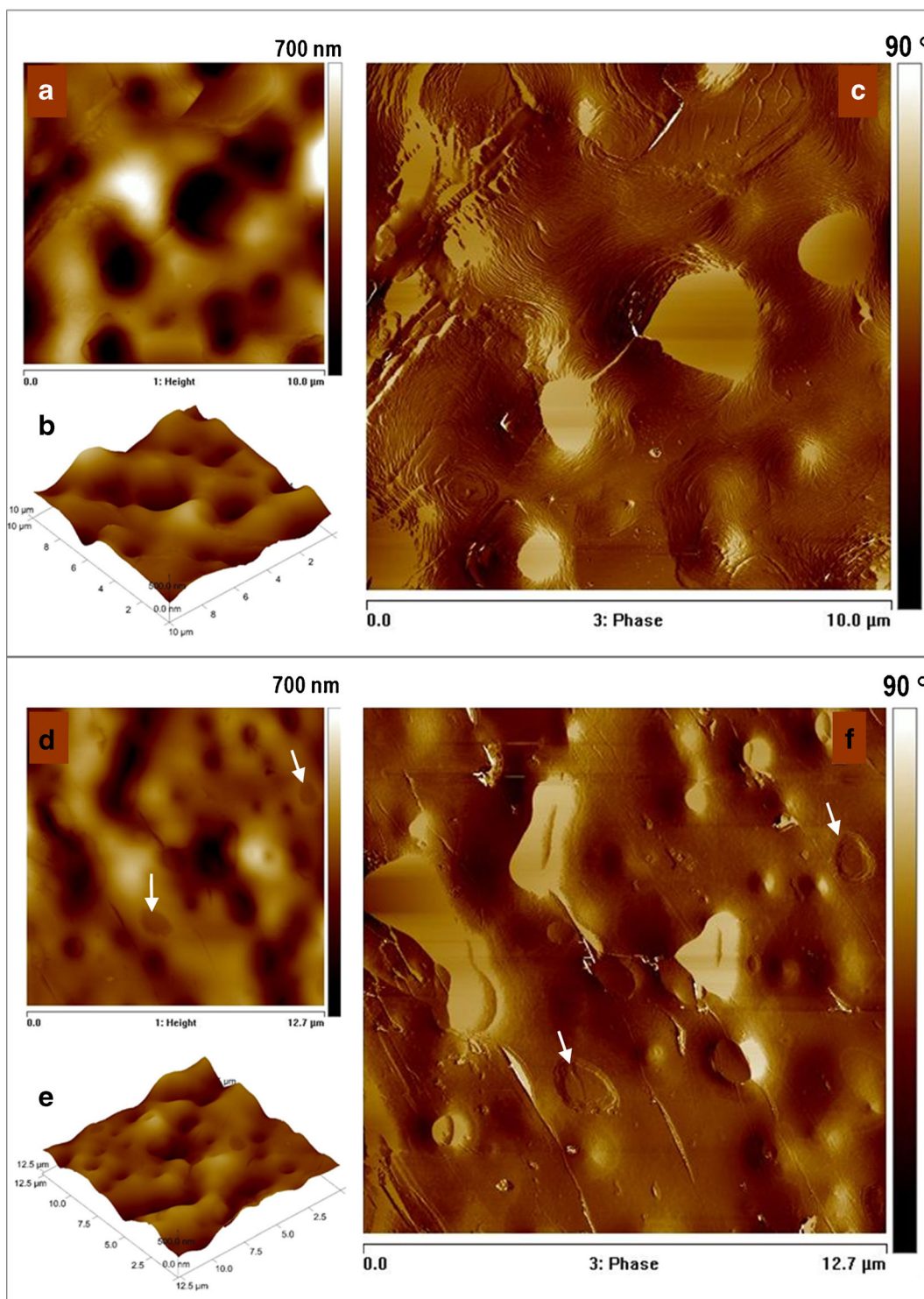


Fig. 5. AFM images of SCN-3 and corresponding MT-loaded SCN-3: (a) 2D- and (b) 3D-views of SCN-3. The scanned area was $10 \times 10 \mu\text{m}$ with z-scale 700 nm. (c) 2D-phase image of the same scanned area with z-scale 90°nm ; (d) 2D- and (e) 3D-views of MT-loaded SCN-3. The scanned area was $10 \times 10 \mu\text{m}$ with z-scale 700 nm. (f) 2D-phase image of the same scanned area with z-scale 90°nm

chemical structure and composition. Here again, SCN-1 and SCN-3 which contain higher PEtOx fractions swell much higher than SCN-2 and SCN-4 (Fig. 1b). Within 5 h, SCN-1 imbibes 800% buffer solution, whereas SCN-2 takes up only

100%. Similarly, SCN-3 reaches 450% swelling in PBS while SCN-4 only reaches 150%. Again, this proves the conclusion that the content of PEtOx is the main factor influencing the SCN swelling in aqueous media.

Drug Loading

The SCNs studied are unique polymer materials with distinctive structure and morphology. The specific feature of these materials, i.e., swelling in aqueous media, was used as a straight way to load MT from solution which ensures preservation of the original network morphology. Highly MT-loaded systems were prepared by immersing the SCN films in concentrated MT aqueous solution and swelling at 20°C until reaching the equilibrium. The results for the MT loading as well as the corresponding MT content in the systems are presented in Table I. The data listed in Table I show that the networks of high PEtOx content (SCN-1 and SCN-3) which swell higher in water exhibit high MT loading capacity (84.19 and 77.26%, respectively). Surprisingly, the networks of lower PEtOx content (SCN-2 and SCN-4) demonstrated relatively high MT loading (64.95 and 64.57%, respectively) despite of extremely low swelling in water. This shows that the extent of swelling of the studied SCNs is not the only parameter influencing their MT loading capacity. It seems that the influence of the hydrophilic–hydrophobic balance in the system is substantial as well. Therefore, the lowest MT loading (46.58%) within the series is observed for the more hydrophobic network, SCN-5.

SEM, DSC, and FTIR Studies

The structure of SCN-3 before and after MT loading was visualized by SEM (Fig. 2). Figure 2a shows micrograph of the fracture of SCN-3 taken in swollen state after freeze-drying. As one can see from the SEM image, the network has smooth walls and well-formed channels. The structure of the MT-loaded system presented in Fig. 2b is significantly changed. The overall morphology is more subtle, and the volume of the channels is significantly reduced. However, the characteristic of MT crystals (Fig. 2c) is not observed here. From the SEM images, it can be concluded that the loaded MT drug is distributed evenly in overall structure of the network and embedded inside the network walls and channels. This is supported by the regular pattern seen on the micrograph (Fig. 2b).

The affinity of MT to the studied networks was further verified by differential scanning calorimetry (DSC) measurements. DSC thermograms of conetworks loaded with MT compared to the thermogram of neat MT are presented in Fig. 3. The melting of the neat MT crystals is observed as a sharp peak at 128°C. In the MT-loaded systems, the start of the melting process is shifted down from 120.4°C for the neat MT to 112.1°C for SCN-1 and further to 89.6°C for SCN-3. This could be assigned to some interaction between the copolymer matrix and the MT or to the changed crystal structure of MT due to its hampered crystallization within the network walls and channels.

Indeed, FTIR spectra confirm the occurrence of such interaction. The ATR-FTIR of the studied SCNs was recorded before and after MT loading (Fig. 4). Comparing the spectra of neat SCNs to these of MT-loaded samples, significant shifts of some bands were registered, most importantly being those of ν C=O band characteristic for the carbonyl groups: from 1,724 to 1,732 cm^{-1} . This is

obviously due to the interaction of carbonyl groups from PHEMA or PHPA segments with MT molecules. In addition, the band at 1,570 cm^{-1} in the MT spectrum assigned to the COO- stretching of tartrate molecule was shifted to 1,512 cm^{-1} in the MT-loaded network.

AFM Studies of the SCNs

The surfaces of the studied SCNs were tested by AFM before and after MT loading. Although the primary SCNs showed differences in the surface roughness, the MT-loaded samples revealed quite similar surface images. Figure 5 presents the detailed AFM investigation of the surface morphology of sample SCN-3, which shows medium swelling in the different solvents and relatively high MT loading. The topography images shown in 2D (Fig. 5a) and 3D (Fig. 5b) format of the SCN-3 reveal a porous structure with an average roughness of about 115 nm. The performed section analysis showed that the depth of the pores was found to vary between 180 and 350 nm. In comparison, the topography images of MT-loaded SCN-3 shown in 2D (Fig. 5d) and 3D (Fig. 5e) format show that the porous structure of the surface is preserved. Moreover, the existence of some depressions on the surface (see arrows at the Fig 5d) with depth of about 30 nm is revealed. These depressions are more profoundly noticeable on the phase image of MT-loaded SCN-3 (Fig. 5f). The nature of these depressions is ambiguous, but it might be assumed that they are a result of the inclusion of the MT in the polymer matrix. The performed analysis showed that the roughness of the surface of MT-loaded SCN-3 is around 90 nm while the depth of the pores was found to vary between 100 and 250 nm.

It is difficult to extract quantitative information from phase images because they are a complex result of a number of parameters and forces acting between the tip and the sample, i.e., adhesion, load force, topography, and the material, especially elastic properties of the sample and so on (32). The comparison of the phase images shows different patterns, which qualitatively implies for the differences in the inner structure and the material properties of the surfaces being investigated.

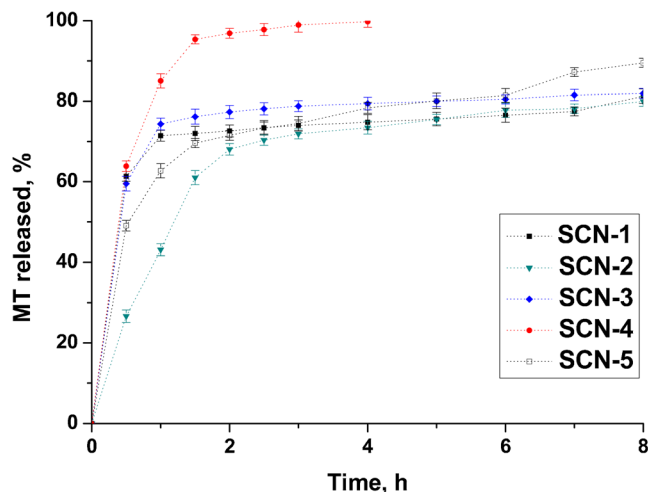


Fig. 6. Release kinetics of MT at pH 6.8 (37°C)

In Vitro Drug Dissolution Studies

MT belongs to BCS Class I drug exhibiting high solubility. It is fully dissolved in the dissolution media (i.e., phosphate standard buffer pH 6.8) within a minute. Figure 6 represents the MT release kinetic curves of the developed systems. The systems SCN-1/MT, SCN-3/MT, and SCN-4/MT although different in chemical composition and structure show high initial MT release rate and discharge more than 60% of the drug within 30 min. After this initial burst effect, the release profiles of these systems differ substantially: the networks SCN-1 and SCN-3 maintain the MT release for 8 h reaching the cumulative MT release of 80%. On the other hand, the network SCN-4 keeps the initial fast release dispensing the entire amount of loaded MT within 5 h. Much slower initial MT release rate is exhibited by SCN-2/MT. As seen in Fig. 6, in this case, only 30% of the MT content is released within 30 min. The sustained MT release from this system continues 3 h dispensing 70% of the loaded drug. At the end of the experiment, 80% of MT is released from SCN-2/MT similarly to SCN-1/MT and SCN-3/MT.

The kinetics of the MT release from PMMA-containing network SCN-5/MT presented in Fig. 6 show that the drug release profile is not influenced significantly by the system hydrophobization. Although this network contains 50 wt.% of water repellent PMMA, the control over the release kinetics is not improved compared to SCN-2/MT. Compared to SCN-1/MT, SCN-3/MT and SCN-4/MT, however, some improvement in the initial MT release rate is observed as only 44% of the loaded drug is released in 30 min. Moreover, it should be emphasized that the altered hydrophilic–hydrophobic balance in this network results in 90% total drug release in 8 h.

The data collected during the *in vitro* drug release experiments were fitted to different kinetic models. Diffusion controlled drug release was confirmed for all studied systems. Values for exponent n lower than 0.35 were obtained when applying Ritger–Peppas model, indicating that quasi-Fickian diffusion (Case I transport) is the dominant drug release mechanism.

From the experimental data obtained, it could be concluded that the copolymer composition and especially the chemical structure the constituents are not determinant of the MT release from the high swelling networks SCN-1 and SCN-3. The MT release properties of the networks of low swelling degree within this series (SCN-2, SCN-4, and SCN-5) however differ drastically. This observation could be explained with the presence or absence of the temperature-responsive PHPA segments in network composition. SCN-4 which is partially collapsed at the experimental conditions applied (PBS; 37°C) provides fast and complete MT release. In contrast, the network SCN-2 which contains highest PHEMA fraction obviously maintains the best sustained MT release within this series. The composition and swelling properties of this network could be further improved and optimized in view of its potential application as carriers for sustained release of MT and other similar hydrophilic drugs.

CONCLUSIONS

Segmented copolymer networks (SCNs) of different composition based on copolymerization of HEMA, HPA, and/or MMA in the presence of PEtOx macromer were studied as

MT delivery systems. The amphiphilic nature of the networks and their capability to swell in aqueous media allowed the effective inclusion of the highly water soluble cardioselective β -blocker metoprolol tartrate in the network structure. Drug delivery systems of 47 to 84 wt.% drug loading were obtained. Both SEM and AFM studies revealed that the loaded MT is uniformly distributed in the whole conetwork structure, whereas the DSC analysis referred to changes in the crystal structure of MT and/or the existence of interaction between MT and polymer matrices. Based on the drug release studies, it can be concluded that all tested networks are able to sustain the MT release without added excipients. The system containing high PHEMA fraction which showed the most effective control over the drug release within these series could be further optimized as promising carrier of MT or other hydrophilic drug molecules.

ACKNOWLEDGMENTS

Financial support by National Science Fund of Bulgaria (Project UNION, Grant # DCVP 02/2/2009) is gratefully acknowledged.

REFERENCES

- Kadajji VG, Betageri GV. Water soluble polymers for pharmaceutical applications. *Polymers*. 2011;3:1972–2009.
- Kelly AM, Wiesbrock F. Strategies for the synthesis of poly(2-Oxazoline)-based hydrogels. *Macromol Rapid Commun*. 2012;33:1632–47.
- Bhadra D, Bahdra S, Jain P, Jain NK. Peggology: a review of PEG-ylated systems. *Pharmazie*. 2002;57:5–29.
- Pasut G, Veronese FM. Polymer drug conjugation, recent achievements and general strategies. *Prog Polym Sci*. 2007;32:933–61.
- Allen TM, Cullis PR. Drug delivery systems: Entering the mainstream. *Science*. 2004;303:1818–22.
- Forster A, Hempenstall J, Rades T. Characterization of glass solutions of poorly water-soluble drugs produced by melt extrusion with hydrophilic amorphous polymers. *J Pharm Pharmacol*. 2001;53:303–15.
- Sairam M, Babu VR, Rao KSVK, Aminabhavi TM. Poly(methylmethacrylate)-poly(vinyl pyrrolidone) microspheres as drug delivery systems: Indomethacin/cefadroxil loading and *in vitro* release study. *J Appl Polym Sci*. 2007;104(3):1860–5.
- Kayal S, Ramanujan RV. Doxorubicin loaded PVA coated iron oxide nanoparticles for targeted drug delivery. *Mater Sci Eng C*. 2010;30:484–90.
- Peppas NA, Mongia NK. Ultrapure poly(vinylalcohol) hydrogels with mucoadhesive drug delivery characteristics. *Eur J Pharm Biopharm*. 1997;43:51–8.
- Ray D, Mohapatra DK, Mohapatra RK, Mohanta GP, Sahoo PK. Synthesis and colon-specific drug delivery of a poly(acrylic acid-co-acrylamide)/MBA nanosized hydrogel. *J Biomater Sci Polym Ed*. 2008;19(11):1487–502.
- Hu Y, Jiang X, Ding Y, Ge H, Yuan Y, Yang C. Synthesis and characterization of chitosan-poly(acrylic acid) nanoparticles. *Biomaterials*. 2002;23:3193–201.
- Liu J, Pang Y, Huang W, Zhu Z, Zhu X, Zhou Y, *et al*. Redox-responsive polyphosphate nanosized assemblies: a smart drug delivery platform for cancer therapy. *Biomacromolecules*. 2011;12:2407–15.
- Pencheva I, Bogomilova A, Koseva N, Obreshkova D, Troev K. HPLC study on the stability of bendamustine hydrochloride immobilized onto polyphosphoesters. *J Pharm Biomed Anal*. 2008;48:1143–50.

14. Adams N, Schubert US. Poly(2-oxazolines) in biological and biomedical application contexts. *Adv Drug Deliv Rev.* 2007;59:1504–20.
15. Schlaad H, Diehl C, Gress A, Meyer M, Demirel AL, Nur Y, *et al.* Poly(2-oxazoline)s as smart bioinspired polymers. *Macromol Rapid Commun.* 2010;31:511–25.
16. Hoogenboom R, Schlaad H. Bioinspired Poly(2-oxazoline)s. *Polymers.* 2011;3:467–88.
17. Kobayashi S, Uyama H. Polymerization of cyclic imino ethers: from its discovery to the present state of the art. *J Polym Sci A Polym Chem.* 2001;40:192–209.
18. Hoogenboom R. Poly(2-oxazoline)s: Alive and kicking. *Macromol Chem Phys.* 2007;208:18–25.
19. Hoogenboom R. Polyethers and polyoxazolines. In: Dubois P, Coulembier O, Raquez JM, editors. *Handbook of ring-opening polymerization.* Weinheim: Wiley-VCH; 2009.
20. Taubmann C, Luxenhofer R, Cesana S, Jordan R. First aldehyde-functionalized poly(2-oxazoline)s for chemoselective ligation. *Macromol Biosci.* 2005;5:603–12.
21. Kowalczyk A, Kronek J, Bosowska K, Trzebicka B, Dworak A. Star poly(2-ethyl-2-oxazoline)s—synthesis and thermosensitivity. *Polym Int.* 2011;60:1001–9.
22. Jin R-H. Water soluble star block poly(oxazoline) with porphyrin label: a unique emulsion and its shape direction. *J Mater Chem.* 2004;14(3):320–7.
23. Christova D, Velichkova R, Goethals E, du Prez FE. Amphiphilic segmented polymer networks based on poly(2-alkyl-2-oxazoline) and poly(methyl methacrylate). *Polymers.* 2002;43:4585–90.
24. Luxenhofer R, Schulz A, Roques C, Li S, Bronich TK, Batrakova EV, *et al.* Doubly amphiphilic poly(2-oxazoline)s as high-capacity delivery systems for hydrophobic drugs. *Biomaterials.* 2010;31:4972–9.
25. Han Y, He Z, Schulz A, Bronich TK, Jordan R, Luxenhofer R, *et al.* Synergistic combinations of multiple chemotherapeutic agents in high capacity poly(2-oxazoline) micelles. *Mol Pharm.* 2012;9(8):2302–13.
26. Guillerme B, Darcos V, Lapinte V, Monge S, Coudane J, Robin J-J. Synthesis and evaluation of triazole-linked poly(ϵ -caprolactone)-graft-poly(2-methyl-2-oxazoline) copolymers as potential drug carriers. *Chem Commun.* 2012;48:2879–81.
27. El-Hag Ali A, AlArifi AS. Swelling and drug release profile of poly(2-ethyl-2-oxazoline)-based hydrogels prepared by gamma radiation-induced copolymerization. *J Appl Polym Sci.* 2011;120(5):3071–7.
28. Kostova B, Ivanova-Mileva K, Rachev D, Christova D. Study of the potential of amphiphilic conetworks based on poly(2-ethyl-2-oxazoline) as new platforms for delivery of drugs with limited solubility. *AAPS Pharm Sci Tech.* 2013;14(1):352–9.
29. Hardman JG, Limbird LE, Gilman AG, editors. *The pharmacological basis of therapeutics.* 10th ed. New York: Mc Graw-Hill Medical Publishing Division; 2001. p. 1125–9.
30. Christova D, Velichkova R, Loos W, Goethals E, Prez F. New thermo-responsive polymer materials based on poly(2-ethyl-2-oxazoline) segments. *Polymers.* 2003;44:2255–61.
31. Christova D, Velichkova R, Goethals EJ. Bis-macromonomers of 2-alkyl-2-oxazolines-synthesis and polymerization. *Macromol Rapid Commun.* 1997;18:1067–73.
32. McLean RS, Sauer BB. Tapping mode AFM studies using phase detection for resolution of nanophases in segmented polyurethanes and other block copolymers. *Macromolecules.* 1997;30:8314–7.